Article

pubs.acs.org/Biomac

Narrow Therapeutic Window of Ribavirin as an Inhibitor of Nitric Oxide Synthesis is Broadened by Macromolecular Prodrugs

Benjamin M. Wohl,[†,‡] Anton A. A. Smith,[†] Mille B. L. Kryger,[†,‡] and Alexander N. Zelikin*[,†,‡]

[†]Department of Chemistry and [‡]iNano Interdisciplinary Nanoscience Centre, Aarhus University, Aarhus 8000, Denmark

Supporting Information

ABSTRACT: Ribavirin (RBV), a broad-spectrum antiviral agent, is a standard medication against hepatitis C virus (HCV). However, despite the decades of clinical success, the mechanism of action of this drug against HCV remains a subject of debate. Furthermore, the appeal of this therapeutic agent is considerably lessened by unfavorable pharmacokinetics. This interdisciplinary study contributes to the understanding of intracellular effects exerted by RBV and presents a successful design of macromolecular prodrugs of RBV to achieve a safer treatment. Specifically, we demonstrate that RBV exhibits a pronounced anti-inflammatory activity in cultured macrophages as is evidenced by a 2-fold decrease in the levels of produced nitric oxide achieved using a clinically relevant concentration of this drug. However, this effect was characterized by a rather narrow therapeutic window with experimental values of EC_{50} and IC_{50} being 7 and 19 μM, respectively. Macromolecular prodrugs were obtained using an acrylate derivative of RBV, RAFT polymerization technique, and *N*-vinyl pyrrolidone as a partner monomer. The synthesized polymers were characterized with uniform molecular weights, relatively narrow polydispersities, and gradually increasing content of RBV. The resulting polymer therapeutics were effective in delivering their payload to the cultured macrophages and afforded a significantly wider therapeutic window, as much as >1000 μM (18-fold in relative values). Taken together, this work contributes significantly to the development of safer methods for delivery of RBV, as well as understanding the mechanism of action and origins of the side effects of this broad-spectrum antiviral agent.

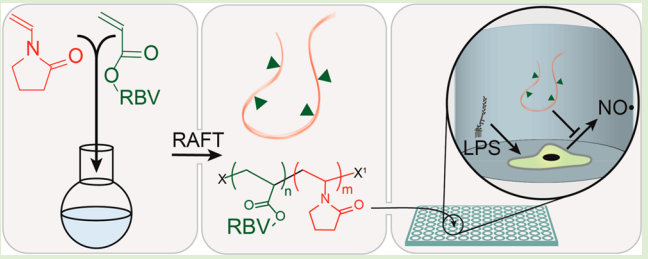

INTRODUCTION

Hepatitis C virus (HCV) is a major health-care challenge, with 130−170 million people being affected worldwide.[1] In a majority of patients, the disease progresses to a chronic infection that remains largely asymptomatic for 20−30 years, while ultimately leading to liver fibrosis, cirrhosis, and liver cancer in 60−70% of the patients, making HCV the leading cause of liver transplantation in western countries.[1,2] Current treatment regimens consist of PEGylated interferon alpha (PEG-IFN-α), ribavirin (RBV), and, as of recently, direct-acting antivirals (DAAs; i.e., viral protease/polymerase inhibitors).[3,4] Treatment efficacies are strongly dependent on the viral genotype and are limited by severe side effects.[5,6]

RBV, a purine nucleoside analog and broad spectrum antiviral against both DNA and RNA viruses, was developed in 1970 and, to this day, remains an indispensable component of antiviral treatment due to its ability to improve the efficacy of both PEG-IFN-α and DAAs.[7−10] Consequently, RBV-associated side effects remain a crucial issue in HCV treatment. Reported effects include fatigue, influenza-like symptoms, gastrointestinal disturbance, neuropsychiatric symptoms, and hematological abnormalities.[6] Accumulation of RBV in red blood cells (RBCs) is due to a facile entry of the drug into these cells through nucleoside transporters. Subsequent intracellular phosphorylation and lack of a mechanism for dephosporylation lead to an entrapment of the drug inside RBCs. This phenomenon results in a depletion of intracellular adenosine triphosphate, oxidative stress on the RBC membrane, and removal of the cell from the bloodstream through the reticuloendothelial system.[11−13] The ensuing hemolytic anemia is a major concern, it severely limits treatment dosages and often requires reduction of drug dose in affected patients,[6,14] whereas in fact higher RBV dosages are required for increased efficacy of treatment.[15]

Despite its success in HCV treatment, the mechanism of action of RBV remains a subject of debate.[7,16] A number of alternative mechanisms have been established to contribute to anti-HCV activity, namely, (i) immunomodulation by enhancing and preserving T_H1 cytokine production, (ii) direct inhibition of the viral NS5B polymerase by binding to the nucleotide binding site, (iii) increased mutational frequency leading to lethal mutagenesis, (iv) modulation of interferon-stimulated gene expression, and (v) inhibition of intracellular inosine-5′-monophosphate dehydrogenase (IMPDH).[17] The direct inhibition of IMPDH by RBV-monophosphate (see Figure 1) results in depletion of intracellular guanosine-5′-triphosphate (GTP), leading in turn to depletion of tetrahydrobiopterin (BH_4), a cofactor required for the

Received: July 18, 2013
Revised: October 3, 2013
Published: October 3, 2013

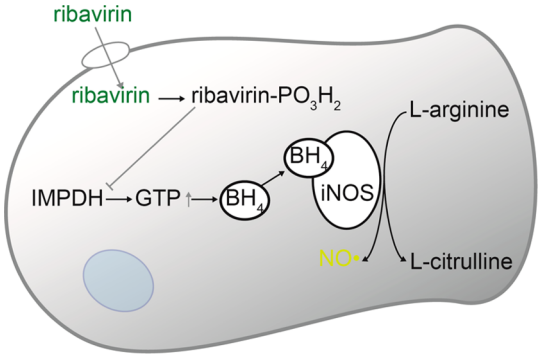

Figure 1. Schematic representation showing the inhibition of NO production through RBV in stimulated macrophages. Following cellular uptake ribavirin (RBV) is phosphorylated to its monophosphate, which is a direct inhibitor of IMPDH, thus leading to depletion of intracellular GTP and in turn depletion of BH_4 pools. BH_4 being an essential cofactor to the performance of inducible nitric oxide.

performance of inducible nitric oxide synthase.[4,18−21] It has been speculated that RBV thus elicits an anti-inflammatory activity which manifests itself through an inhibition of nitric oxide (NO) production. This effect might have direct relevance to anti-HCV treatment as it has been hypothesized that virus-induced up-regulation of NO levels mediates pathogenic activity and also favors viral persistence.[22,23] In fact, known IMPDH inhibitors that exhibit activity on BH_4 and NO levels, such as mycophenolic acid, are currently being investigated for their anti-HCV activity.[4,24] Surprisingly, the RBV-iNOS connection was verified in a solitary report, in endothelial cells, with relevance to angiogenesis[19] and has not been tested in cell culture with relevance to hepatic applications. In our previous publication[25] we revealed that, taken at clinically relevant concentration (10 μM), ribavirin indeed inhibits production of nitric oxide in LPS-stimulated macrophages, the latter serving as models for liver resident Kupffer cells. We believe that given the broadness of application of RBV in clinic, a detailed characterization of this intracellular target is highly warranted, and this was the objective of the study presented herein.

The further aim of this work was to investigate opportunities toward improvement of pharmacokinetics of RBV using macromolecular prodrugs (MPs), that is, polymer−drug conjugates.[26] The utility of MPs is well established in anticancer therapy and accomplishments of this field are highlighted by several formulations having progressed to advanced clinical trials.[26] Surprisingly, developments of polymer therapeutics in the area of antiviral therapy are modest,[27−36] and examples of polymer conjugated formulations of RBV are solitary.[34,37−39] Li et al. reported a galactose-rich, RBV-functionalized copolymer system that self-assembled into micelles, underwent internalization by hepatic cells, and released pristine RBV over time.[34,38] However, a therapeutic benefit of these formulations was not established. Brookes et al. reported the synthesis of a hemoglobin−RBV conjugate through a phosphoramidate linkage on the 5′-hydroxyl of RBV.[37] These bioconjugates demonstrated enhanced antiviral activity in both hepatocytes and macrophages isolated from a viral hepatitis mouse model. In vivo results from this system showed that both free RBV and hemoglobin−RBV conjugates enhanced survival rates compared to nontreated mice. However, while mice treated with free RBV developed lethargy and abnormal fur texture, treatment with hemoglobin−RBV resulted in no such side effects.[37] Furthermore, it was demonstrated that RBV and its conjugates decreased the production of interferon-γ and tumor necrosis factor-α (i.e., an anti-inflammatory activity), as well as improved liver histology and function (i.e., reduced alanine transaminase levels). A lactosaminated poly-L-lysine RBV conjugate reported by Di Stefano et al. further demonstrated the potential benefits associated with liver targeted MPs by showing increased drug efficiency and a significant increase in the liver/erythrocyte ratio between free drug and conjugate.[39,40]

Recently, we reported that poly(acrylic acid), PAA, and poly(vinyl pyrrolidone), PVP, can be used as carrier polymers to bypass association with erythrocytes and at the same time achieve efficient delivery of RBV to mammalian cells with hepatic relevance, hepatocytes and macrophages.[25,41] Encouraged by these findings, in this work we focus on PVP and further investigate therapeutic benefits achieved through polymer-assisted delivery of RBV to cultured macrophages. PVP is a polymer with an extensive history of biomedical applications and excellent biocompatibility, as illustrated by its former use as a plasma expander.[42] However, only solitary examples of PVP used as a drug carrier have been reported.[42,43] In part, this is due to the challenging nature of the monomer and poor opportunities in the production of copolymers of NVP with (meth-)acrylate monomers. Over the past few years, we explored the synthesis of PVP via RAFT polymerization technique[44] and the use of this polymer in bioconjugation strategies.[45,46] Herein, we use RAFT polymerization to obtain well-defined polymer conjugates with increasing content of RBV and investigate in detail the changes in the therapeutic window of treatment afforded by PVP-based macromolecular prodrugs as compared to that of the pristine drug.

MATERIALS AND METHODS

All chemicals were ordered from Sigma-Aldrich and used as received, if not indicated otherwise. Water used throughout this work was of Milli-Q quality (18.2 MΩ·cm, Millipore Milli-Q Direct 8). Mass spectrometry (MS-ESI) was performed on a Bruker maXis Impact. Fluorescence and absorbance measurements were conducted on an Enspire Perkin-Elmer plate reader. NMR spectra were recorded on a Varian Mercury 400 NMR. Chemical shifts are reported in ppm in relation to an external tetramethylsilane standard. Candida Antartica lipase (Nz435) enzyme beads were a kind gift from Novozymes, Denmark.

Synthesis of RBV Acrylate. Ribavirin (Tokyo Chemical Industry, 20 mg, 0.082 mmmol) was suspended in 0.8 mL of dioxane together with the enzyme beads (Nz435, 100 mg) and a few crystals of di-*tert*-butyl methylphenol. After the addition of acetoneoxime acrylate (73 mg, 0.57 mmol), the mixture was stirred at 50 °C for 32 h. The reaction mixture was reduced and purified by column chromatography with 20:80 MeOH/EtOAc to afford RBV-5-*O*-acrylate as a white powder (17 mg, 0.057 mmol, 69%). ^{1}H NMR (DMSO-d_6), δ (ppm): 8.80 (s, 1H, -N=CH-), 7.81 (s, 1H, -NH_2), 7.61 (s, 1H, -NH_2), 6.32 (dd, 1H, J = 4 Hz, J = 16 Hz, CH_2=), 6.13 (dd, 1H, J = 12 Hz, J = 16 Hz, CH_2=), 5.90 (dd, 1H, J = 4 Hz, J = 12 Hz, J = 4 Hz, =CH-), 5.88 (s, 1H, N-CH-O), 5.65 (s, 1H, 3′-OH), 5.38 (s, 1H, 2′-OH), 4.25 (m, 5H, -CH_2-, -CH-O, -CH-O). ^{13}C NMR (DMSO-d_6), δ (ppm): 165.71 (C=O), 160.75 (C3), 158.01 (C6), 145.90 (C5), 132.39 (CH_2=), 128.40 (=CH-), 91.87 (1′C), 81.85 (4′C), 74.59 (2′C), 70.80 (3′C), 64.48 (5′C). MS-ESI: 298.0913.

Synthesis of PVP-RBV6%. RBV-acrylate (24.0 mg, 80.5 μmol), phthalimidomethyl-*O*-ethyl xanthate (RAFT agent, 5.0 mg, 18 mmol), and azobisisobutyronitrile (initiator, 0.26 mg, 1.60 mmol) were dissolved in 0.67 mL of DMSO. After the addition of *N*-vinyl pyrrolidone (360 mg, 3.24 mmol), the solution was degassed through four freeze−pump−thaw cycles. The reaction was left to proceed for

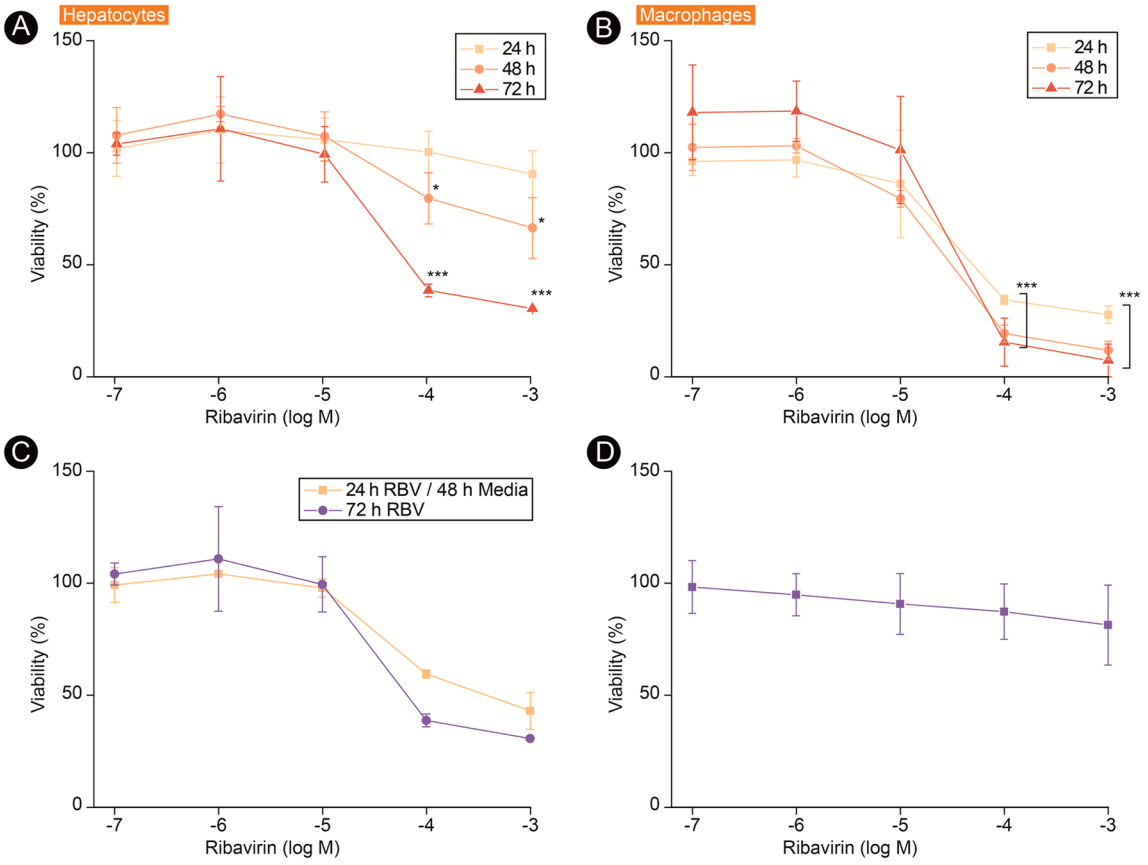

Figure 2. Time- and dose-dependent toxicity of ribavirin in Hep G2 (A) and RAW264.7 (B) cells. Cytotoxicity in Hep G2, comparing 24 h with RBV and 48 h without RBV, to 72 h with RBV (C). Toxicity of ribavirin in confluent RAW264.7 cells after 24 h (D). Results shown are the average of three independent experiments, reported as mean ± SD (n = 3). Statistical significance is given compared to the negative control. *P < 0.05, ***P < 0.001.

23 h at 60 °C, followed by precipitation into diethyl ether to obtain the product (140 mg). ^{1}H NMR ($(CD_3)_2SO$), δ (ppm):): 8.80 (bs, 1H, -N═CH-), 7.81 (bs, 1H, -NH_2), 7.61 (bs, 1H, -NH_2), 5.88 (bs, 1H, N-CH-O), 5.65 (bs, 1H, 3′-OH), 5.38 (bs, 1H, 2′-OH), 4−4.4 (bm, m, 5H, -CH_2-, -CH-O, -CH-O, -CH-), 2.8−3.8 (broad signal, PVP polymer, 3H), 1.2−2.3 (broad signal, PVP polymer, 6H). Phthamidyl terminal group protons from the RAFT agent overlaps with 7.81 (bs, 1H, -NH_2) giving rise to the abnormal intensity of this peak. Polymer samples of varying RBV content were obtained by adjusting the RBV feed accordingly. For cell experiments PVP polymers were dissolved in a minimal volume of DMSO (i.e., 3 μL), followed by dilution with media to the desired concentration. Final DMSO concentrations had no activity in the used assays.

Polymer Characterization. Gel permeation chromatography (GPC) was performed on a system comprising a LC-20AD Shimadzu HPLC pump, a Shimadzu RID-10A refractive index detector and a DAWN HELEOS 8 LS detector. PVP polymers were analyzed on a Mz-Gel SDplus Linear column (MZ-Analysetechnik, L 300 mm, ID 8 mm, 5 μm particles, effective MW range 1000−1000000) using DMF with 10 mM LiBr as eluent at 30 °C (flow rate: 1 mL/min). The dn/dc used in the mass calculations was 0.095 mL/g. The RBV-content was calculated from the intensity of the 5.9 ppm peak in the ^{1}H NMR from RBV compared to the multiplet 1.2−2.4 ppm corresponding to 6 protons in the polymer backbone, see Supporting Information, Figure 5.

Cell Culture. Hep G2 (human liver carcinoma) cells were maintained in Minimum Essential Medium Eagle (MEME) supplemented with Fetal Bovine Serum (FBS, 10%), penicillin streptomycin (P/S, 1%), nonessential amino acids (NEA, 1%), and L-glutamine (2 mM) at 37 °C in 5% CO_2. Cells were routinely passaged using trypsin-EDTA (0.05%). RAW 264.7 (ECACC, murine monocyte macrophage) cells were maintained in Dulbecco's modified Eagle's medium (DMEM), FBS (10%), and P/S (1%) at 37 °C in 5% CO_2. Cells were routinely passaged with a cell scraper.

Cytotoxicity of RBV and MPs in Hep G2 and RAW264.7. Hep G2 cells (50000 cells/well, for 24 h, 20000 cells/well for 48 h, and 10000 cells/well for 72 h, 100 μL media) and RAW264.7 macrophages (20000 cells/well for 24 h, 10000 cells/well for 48 h, and 5000 cells/well for 72 h, 100 μL media) were seeded in 96-well multiplates and left to adhere for 24 h. Media was refreshed (90 μL) and substrate added (10 μL). After respective incubation times viability was measured via CCK-8 (10 μL, 1 h, abs. 450 nm). Viability was normalized against the negative control (10 μL PBS). Positive control: 50% DMSO.

Hemolysis and Agglutination Assay. Human RBCs (Skejby Hospital blood bank, Denmark) were washed and mixed with a cryopreservative (54.7 mM glycerol, 0.050 M $NaPO_3$, 0.37 mM NaCl) and stored at −80 °C previous to experiments. A total of 45 μL of freshly thawed and washed (PBS, 3× 10 mL, 5 min, 400 rpm) RBCs were added to a 96-well multiplate and subjected to polymers (5 μL). A blank (untreated cells), negative control (PBS), and positive control (50% Milli-Q water) were included. RBC suspensions were incubated while shaking overnight (37 °C, 300 rpm). After incubation PBS (150 μL) was added gently, followed by centrifugation (5 min, 400 rpm). A total of 50 μL of supernatant was then transferred to a new 96-well multiplate, absorbance was quantified (541 nm) and relative hemolysis calculated through normalization to the positive control. The remaining cell suspension was diluted 1:1000 with PBS for analysis through flow cytometry (10000 events/sample).

Nitric Oxide Assay. RAW264.7 cells were seeded (20000 cells/well, 100 μL) in 96-well plates. Substrates were added according to the respective timeframes. Time point: −24 h marks 2−3 h after cell

dx.doi.org/10.1021/bm401048s | Biomacromolecules 2013, 14, 3916−3926

seeding, when complete attachment of the cells to the surface was observed. Throughout the experiments media was refreshed every 24 h. Concentrations of small molecular weight compounds (e.g., RBV) in the cell media were kept constant throughout the experiment, while polymers were added once at the specified time point. For LPS stimulation media was refreshed (DMEM phenol-red free) and macrophages were stimulated through the addition of LPS (*E. coli* 026:B6, 1 μg/mL). After a further 24 h incubation, 50 μL of media was transferred to a new multiplate for nitrite determination via the Griess assay. A total of 50 μL of sulfanilic acid (10 g/L, 5% phosphoric acid) was added to each well. After a 5 min incubation, 50 μL of *N*-(1-napthyl)ethylenediamine dihydrochloride (1 g/L, water) was added. After a further 5 min incubation, absorbance (548 nm) was measured, and nitrite levels quantified against a freshly prepared sodium nitrite standard curve. Nitrite concentrations were normalized against the negative control (only LPS) to yield relative nitric oxide levels. Positive control: 1 mM L-N^G-nitroarginine methyl ester (L-NAME). In a typical experiment 24 h LPS stimulation resulted in 20 μM nitrite. In the original cell-containing plate media was refreshed (100 μL) and viability assayed through the addition of PrestoBlue (Invitrogen, 10 μL, 30 min incubation at 37 °C, excitation 560 nm, emission 590 nm). Viability was normalized to the negative control (10 μL PBS). Positive control: 20% DMSO.

Dynamic Light Scattering (DLS). Samples for DLS were prepared analogous to cell culture experiments in PBS. An initial experiment revealed no significant size difference between particles in PBS, DMEM, and DMEM + FBS.

Data Analysis. Obtained results were analyzed in Mircosoft Excel 2010 and plotted in OriginPro (Origin Lab, v.8.5). EC_{50} and IC_{50} values were calculated in OriginPro based on a dose−response fitting function. Statistical significance was demonstrated through a two-tailed heteroscedastic T-Test (Excel) and was considered significant if $P < 0.05$ (*), $P < 0.01$ (**), and $P < 0.001$ (***).

RESULTS AND DISCUSSION

Ribavirin is a powerful member in an arsenal of antiviral drugs and remains one of very few available broad-spectrum antiviral therapeutics.[7] With this in mind, it is highly surprising that the mechanism of action of RBV against HCV is poorly understood, as are the origins of associated side effects. In the process of development of controlled release formulations for this drug, we faced a challenge to ascertain the success of RBV delivery and realized that as of yet, there are no readily available screens for intracellular activity of RBV in virus-free cell culture. Literature survey identified a hypothesis that being an inhibitor of IMPDH (in its phosphorylated form), RBV is expected to deplete the intracellular pool of tetrahydrobiopterin (BH_4) and, in doing so, to decrease the production of nitric oxide. Surprisingly, to the best of our knowledge, the RBV−nitric oxide connection has not been verified in macrophages. With that, nitric oxide is a secretable radical with a lifetime in aqueous solutions not exceeding few seconds with products of degradation (nitrate, nitrite) being readily measurable anions.[47]

Time-Dependent Toxicity in Hepatocytes and Macrophages. To (dis)prove anti-inflammatory activity of RBV, we used two cell lines which are accepted as models for hepatic cells, hepatocytes, Hep G2, and macrophages, RAW264.7.[48,49] In the first set of experiments, we aimed to define the time−concentration parameter space and reveal potential cytotoxic effects of RBV. Mammalian cells were subjected to a wide range of RBV concentrations and metabolic activity, commonly accepted to be indicative of viability, was assayed after 24, 48, and 72 h, Figure 2A,B. Following 72 h incubation, the drug revealed an expected dose-dependent cytotoxicity profile with IC_{50} values close to 30 μM for both, hepatocytes and macrophages. We note that reported values of therapeutic concentration of RBV in the patients plasma, 9−18 μM,[50] are rather close to the revealed toxic concentration and this is an early indicator of a narrow therapeutic window of RBV. This notion will be discussed in detail below.

A surprising finding seen from Figure 2A,B is that toxicity of RBV manifests itself in macrophages significantly earlier than in hepatocytes. Indeed, toxicity in macrophages was equally pronounced following 24, 48, and 72 h of incubation with the drug and revealed very similar values of IC_{50} (26, 30, and 28 μM, respectively). In stark contrast, 24 h incubation of hepatocytes with RBV led to only marginal cytotoxic effects even when the drug was taken in mM concentrations. To probe if the latter effect is due to suppressed or delayed uptake of the drug, the cells were incubated with RBV during an entire 72 h incubation or over 24 h followed by a 48 h culture in drug free media. Resulting toxic effects were similar (Figure 2C), thus, strongly suggesting that time-delayed activity of the drug is likely due to intracellular processes (trafficking and metabolism of RBV, as well as downstream signaling and metabolic pathways) rather than cell entry kinetics. Also of interest, cytotoxicity of RBV in macrophages was suppressed to negligible levels when tested in near-confluent culture, Figure 2D. This possibly indicates that toxicity of RBV in this cell line is directly related to proliferation of cells. Together, data in Figure 2 suggest that intracellular fate, metabolism, and activity of RBV in hepatocytes and macrophages is significantly different, possibly implying that the origin of cytotoxicity in these two cells lines is also different. At present, we cannot offer plausible explanation to the revealed phenomena and understanding of these observations requires further experimentation well exceeding the scope of this manuscript.

Anti-Inflammatory Activity of RBV in Stimulated Macrophages. Anti-inflammatory activity of RBV was ascertained in murine macrophages stimulated with a potent pro-inflammatory agent, lipopolysaccharide (LPS). Twenty-four hours after addition of LPS, relative NO levels and cell viability were determined through the Griess assay[47] and a commercial viability assay, respectively, Figure 3. When administered simultaneously with LPS, therapeutically relevant doses of RBV (∼10 μM) led to an *increased* production of NO and at 100 μM RBV relative levels of this inflammatory marker reached 150%. This observation contrasts with the expected anti-inflammatory effect of RBV, but agrees with the previously reported induction of NO synthesis by nucleoside analogues, possibly through the interaction with the purine P1 receptor.[51] Nevertheless, with this mode of drug administration, inhibition of NO production was possible with RBV yet it required millimolar concentrations of the drug, well exceeding the therapeutic plasma drug content. This effect was also associated with a statistically significant cytotoxicity. In contrast to the observations discussed above, administration of RBV 24 h prior to macrophage stimulation resulted in a clear dose-dependent inhibition of production of NO, Figure 3B. Preincubation with as little as 1 μM RBV resulted in a statistically significant anti-inflammatory effect with no associated toxicity. Increase in RBV concentration resulted in a gradual enhancement in suppression of NO production, but also an increasingly pronounced cytotoxic effect. Experimental data revealed an EC_{50} value of 7 μM, which is in close agreement with clinical concentrations of this drug, (9−18 μM),[50] and a viability associated IC_{50} value of 19 μM. Increasing the preincubation time to 48 h did not significantly enhance the activity of RBV (see Supporting Information, Figure 1). These data reveal that RBV exhibits a

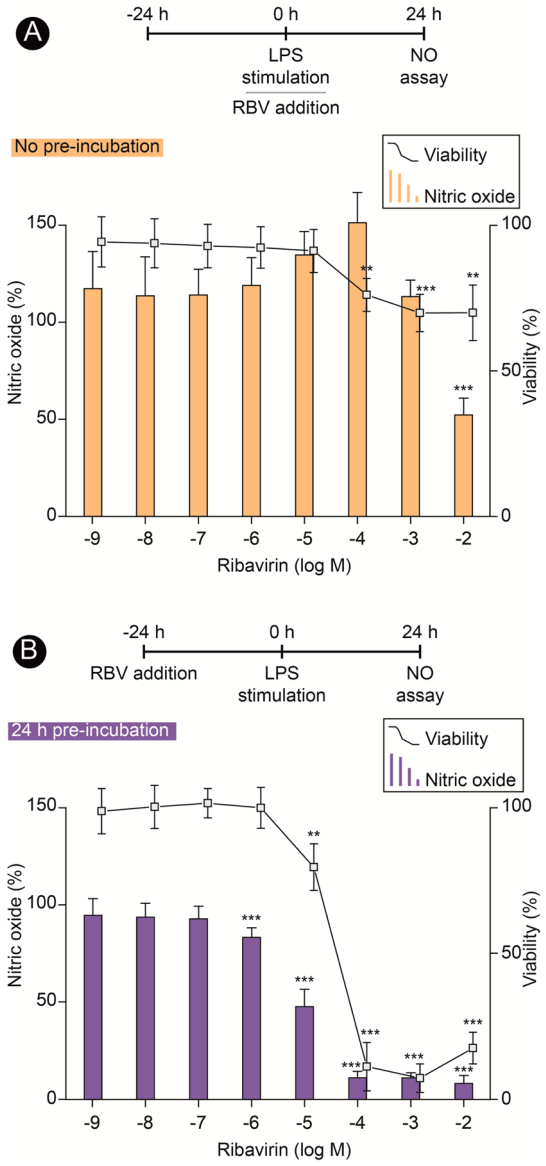

Figure 3. Dose-dependent toxicity and inhibition of nitric oxide production in LPS-stimulated RAW264.7 cells by ribavirin. Cell were stimulated simultaneously with RBV addition (A) or preincubated with RBV for 24 h followed by stimulation (B). Results shown are the average of three independent experiments, reported as mean ± SD (n = 3). L-N^G-nitroarginine methyl ester (L-NAME, 1 mM), a potent NO inhibitor,[58] resulted in 80 ± 2% NO reduction without toxicity. Statistical significance is given compared to the negative control. *P < 0.05, **P < 0.01, ***P < 0.001.

clear anti-inflammatory activity and does so at concentrations close to the therapeutic dose. This observation implies that anti-inflammatory activity of RBV is likely to manifest itself in clinic. Our data further illustrate that for this effect, the therapeutic window is remarkably narrow, Figure 4, a notion which has to be taken into account in optimization of therapy regimen, as well as the design of novel prodrugs of ribavirin

Synthesis of Macromolecular Prodrugs of Ribavirin (RBV-MPs). To achieve the synthesis of MPs of RBV, we previously developed a polymerizable RBV derivative, RBV acrylate.[25] Esters are among the most widely employed functionalities in the design of prodrugs and are amenable for both, hydrolytic and enzymatic degradation to liberate pristine

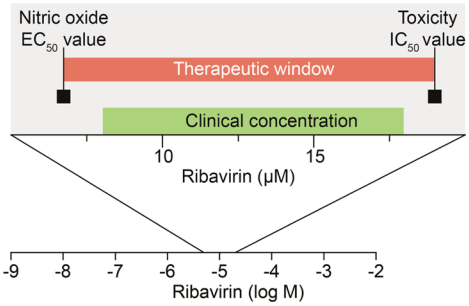

Figure 4. Ribavirin shows inhibition of nitric oxide production and toxicity at clinical concentrations in LPS-stimulated macrophages at 24 h preincubation.

drug.[52] Further, in contrast to the previously described vinyl esters of RBV,[34] acrylates are amenable for copolymerization with a wide variety of monomers and thus provide broader opportunities in macromolecular design. RBV acrylate was synthesized via a chemi-enzymatic pathway, as illustrated in Figure 5, using solid support-immobilized lipase enzyme,

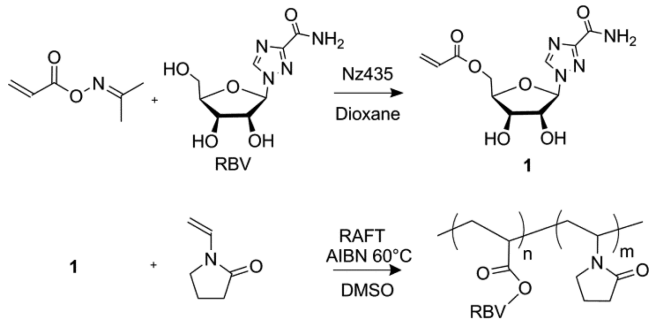

Figure 5. Synthesis of ribavirin acrylate monomer through a chemi-enzymatic pathway (top). RAFT controlled copolymerization of RBV acrylate with *N*-vinyl pyrrolidone (NVP) to afford macromolecular prodrugs of RBV (bottom). Phthalimidomethyl-*O*-ethyl xanthate was employed as RAFT agent (see Supporting Information, Figure 3).

Novozyme 435. This synthetic approach is significantly advantaged over chemical pathways in that the latter require the use of protective group schemes, are labor intensive, and afford lower yields of target compounds.

For polymer synthesis, we employed the RAFT polymerization technique with its capabilities to synthesize polymer samples with controlled molecular weights and narrow polydispersities. NVP underwent copolymerization with RBV acrylate with a near quantitative incorporation of the drug-equipped monomer into the polymer backbone. This is readily explained by a higher reactivity of acrylates toward polymerization, as well as the choice of the xanthate RAFT agent. The latter provides good control over polymerization of NVP, however, through increased rates of fragmentation affords ill-controlled polymerization of acrylates. Nevertheless, at low to moderate feed of RBV acrylate in the monomer mixture, polydispersity indexes of the polymers were significantly lower than those typically reported for NVP copolymers used in drug delivery.[53,54] Final PVP polymer library was characterized with molecular weights 6−13 kDa, that is, favoring renal secretion of the polymers, and RBV content varied from 2 to 9 mol %, see Figure 6 and Supporting Information, Table 1. NMR spectra of macromolecular prodrugs indicated successful incorporation of the drug into the polymer and also demonstrated that the

dx.doi.org/10.1021/bm401048s | *Biomacromolecules* 2013, 14, 3916−3926

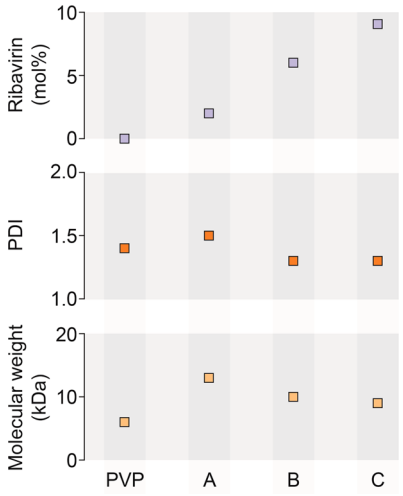

Figure 6. Characteristics of PVP-RBV polymer library prepared via RAFT polymerization. Also see Supporting Information, Table 1.

samples did not contain residual drug or acrylate monomer (Figure 7), at least with the precision of this spectroscopy technique.

Hemocompatibility of the RBV-MPs. As the first test for the synthesized macromolecular prodrugs of RBV, we aimed to validate their hemocompatibility. Previously, we have shown that macromolecular prodrugs of RBV overcome the main side effect of RBV, namely, accumulation in red blood cells.[25,41] We also demonstrated that the polymers exhibit no hemolytic activity and do not cause aggregation of erythrocytes. However, the polymers synthesized herein covered a broader range of RBV drug content and we aimed to verify the properties of these MPs with regard to hemolysis and hemagglutination of erythrocytes. Overnight incubation of RBCs in the presence of 0.1 g/L of RBV MPs resulted in no measurable hemolysis as quantified through UV−vis absorbance of released hemoglobin, Figure 8. Aggregation of the erythrocytes was quantified using flow cytometry and specifically the light scattering characteristics of the cells populations.[55] Aggregation phenomena result in a significant increase in light scattering and a corresponding shift of the events to higher FSC/SSC values. In the experiments with RBV-MPs, no significant differences in the

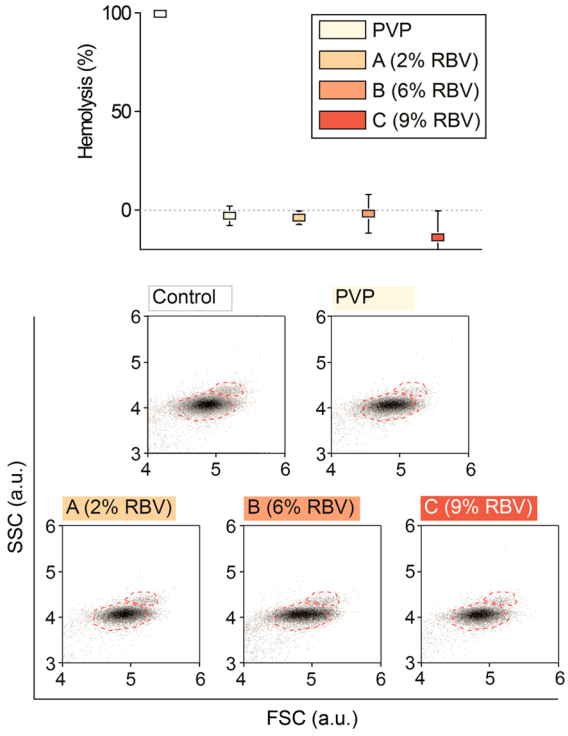

Figure 8. Hemolysis (top) and hemagglutination (bottom) induced by the presence of RBV MPs. Hemolysis was quantified through the UV−vis measurements of released hemoglobin and reported as mean ± SD of three independent experiments (n = 3). Hemagglutination was analyzed by flow cytometry; data shown in scatterplots are representative and were reproduced in three independent experiments.

light scattering parameters were identified between populations of erythrocytes incubated in PBS or in the presence of MPs thus demonstrating hemocompatibility of the synthesized prodrugs.

Intracellular Activity of RBV-MPs. Next, we ascertained toxicity of these polymers in cultured hepatocytes, Figure 9. Polymer toxicity can be inherent with the polymer chemistry, due to the conjugated drug, or be associated with the RAFT agent-derived terminal groups.[56,57] From a different perspective, several previously reported macromolecular prodrugs of

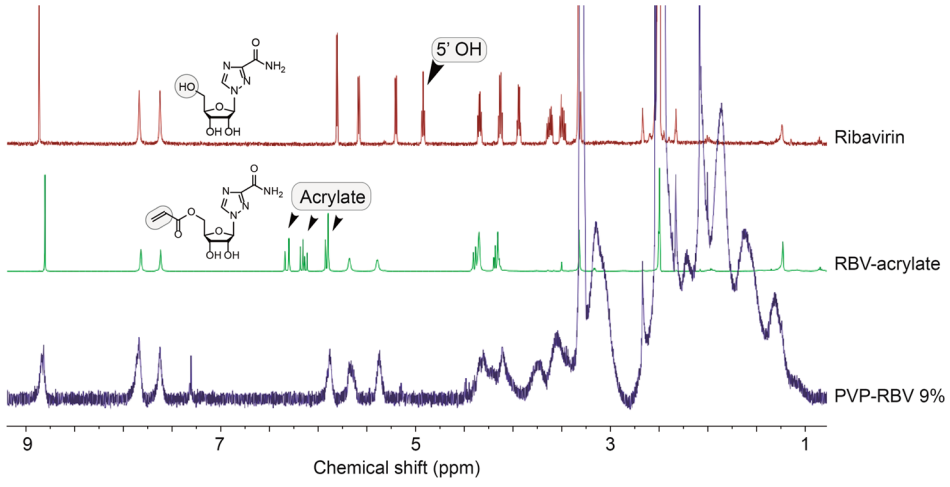

Figure 7. Comparison of ^{1}H NMR spectra of ribavirin, ribavirin-acrylate, and PVP-RBV 9 mol % showing disappearance of the signal from the 5′-hydroxyl upon formation of RBV-acrylate and similarly the disappearance of the signal from the acrylate groups during polymerization.

dx.doi.org/10.1021/bm401048s | Biomacromolecules 2013, 14, 3916−3926

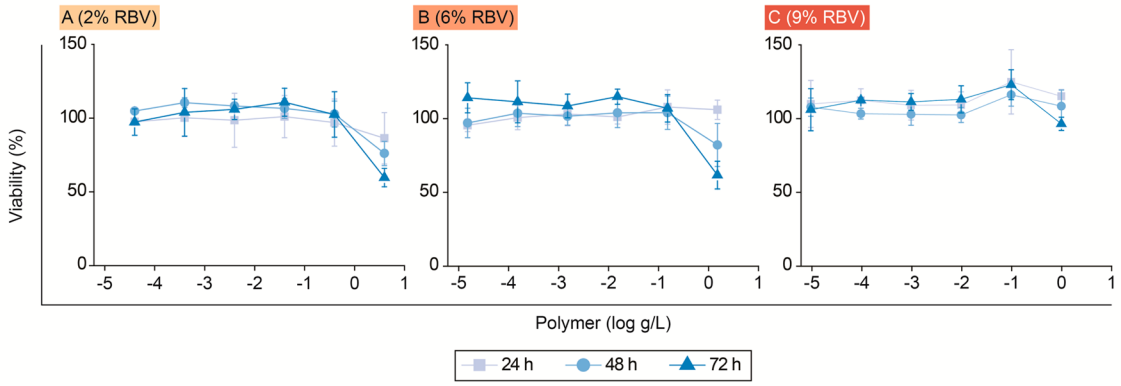

Figure 9. Viability of Hep G2 cells incubated with PVP-RBV copolymers for 24, 48, and 72 h. Results shown are the average of three independent experiments, reported as mean ± SD (n = 3).

RBV have been characterized with regard to the drug activity only through the measurements of cytotoxicity of the prodrugs in hepatocytes.[34,37,38] For direct comparison, we aimed to evaluate the newly synthesized polymers in a similar assay. Hepatocytes were incubated with increasing concentrations of the polymers over a wide range of concentrations and time of incubation of up to 72 h. RBV-MPs exhibited an excellent safety profile and administration of polymer therapeutics in concentrations up to ~1 g/L exerted no detrimental effect on the proliferation of hepatocytes, Figure 9. We note that any drug-associated toxicity is a highly unfavorable side effect in antiviral treatment. This is in contrast to anticancer agents where toxicity, albeit limited to the target tissue, is highly warranted. Data in Figure 9 suggest that high levels of free RBV can only be delivered at high polymer concentrations. At the same time, a therapeutic response might be achieved at much lower concentrations that do not register in a purely cytotoxic assay, and this indeed was observed in the experiments presented below.

To ascertain therapeutic benefits associated with the use of macromolecular prodrugs of RBV, we made use of the above-established assay and quantified anti-inflammatory response achieved by PVP-RBV conjugates in LPS-stimulated macrophages. In the initial experiment, we aimed to compare polymer conjugates to the pristine drug taken at a concentration close to its therapeutic value (10 μM), a direct inhibitor of iNOS L-NAME,[58] and pristine polymer, PVP. Macromolecular prodrugs were administered onto cultured macrophages at a 0.1 g/L concentration 24 h prior to stimulation with LPS. Following additional 24 h of incubation, levels of NO and cell viability were quantified, Figure 10.

In this experiment, a competitive inhibitor of iNOS (L-NAME) afforded a near 80% inhibition of production of NO. Pristine polymer, PVP, revealed no activity or associated cytotoxicity and both NO and viability remained on ~100%. In contrast, each of the three RBV-MPs showed a statistically significant decrease in the levels of nitric oxide. At this polymer concentration, polymer conjugates afforded 30−50% decrease in the level of NO and for the conjugate with 6 mol % RBV, inhibition of NO production was as pronounced as for the pristine drug. In our previous publication, a PVP-RBV conjugate administered at conditions identical to those in Figure 10 afforded only a 25% inhibition of NO synthesis.[41] The polymer series in this work was characterized with consistently lower molecular weight, potentially favoring cellular internalization and, thus, possibly leading to higher

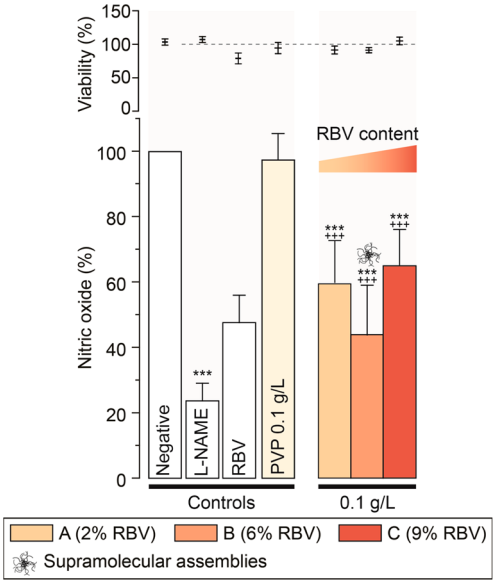

Figure 10. Inhibition of nitric oxide production in LPS-stimulated RAW 264.7 cells by RBV-MPs and accompanying cell viability. Results shown are the average of six independent experiments, reported as mean ± SD (n = 6). Statistical significance is given compared to the negative control (*) or compared to the pristine PVP control (+). ***,+++P < 0.001.

therapeutic effects. Considering the fact that RBV's inhibitory activity on IMPDH requires intracellular phosphorylation on the same 5′-hydroxyl as used in the synthesis of MPs,[16] presented data strongly suggest that the synthesized MPs afford efficient intracellular release of RBV. The studied polymer concentrations correspond to 17, 49, and 70 μM total RBV content in MPs A, B, and C, respectively. However, MPs exhibited cytotoxicity not exceeding that of the pristine polymer (cell viability > 90%). This observation implies that attained intracellular drug concentration is sufficient for therapeutic response but does not exceed the threshold for toxicity.

Interestingly, data in Figure 10 demonstrate that the highest therapeutic effect of PVP-RBV conjugates in the anti-inflammatory assay in cultured macrophages was not attained with the polymer with the highest content of RBV. Indeed, MP with 6 mol % RBV exhibited a higher inhibition of NO synthesis as compared to the conjugates with 2 and 9 mol % of the drug containing monomer. The conjugate with the highest

dx.doi.org/10.1021/bm401048s | Biomacromolecules 2013, 14, 3916−3926

activity was also the only MP that revealed supramolecular assemblies in aqueous solution. Dynamic light scattering experiments using 0.1 g/L solution of this copolymer registered well-defined assemblies sized ~200 nm (polydispersity 0.235). At present it is unclear as to why the 2 mol % and especially the 9 mol % RBV conjugates do not reveal this behavior. It is also important to note that supramolecular assemblies of PVP-RBV appear to be highly labile and our attempts to visualize these aggregates using a transmission electron microscope were met with failure. However, data in Figures 10 and 11 suggest that micellization may prove an advantageous characteristic for macromolecular prodrugs of RBV.

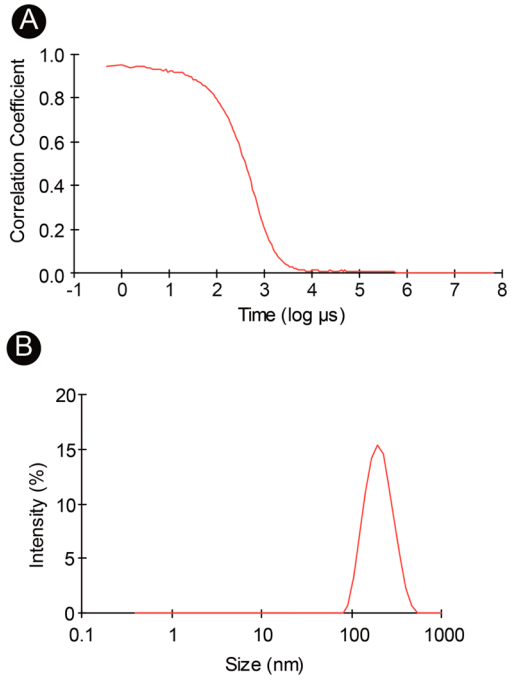

Figure 11. (A) Representative correlation function and (B) size measurement obtained via DLS on PVP-RBV MP with 6 mol %.

Pharmacodynamics of RBV-MPs. Encouraged by the data in Figure 10, we aimed to define the therapeutic window made possible by the polymer-conjugated preparation of RBV. To achieve this, the synthesized polymers were administered onto cultured macrophages using a wide range of polymer concentrations, ranging from 10 μg/L to 1 g/L. Following 24 h incubation with polymers, the cells were stimulated with LPS and after an additional 24 h, levels of NO were quantified along with cell viability, Figure 12.

In the entire range of concentrations, pristine PVP exhibited no effect on the rate of proliferation of the cells or the levels of produced nitric oxide. In contrast, RBV-containing polymers with each of the three loadings showed a dose-dependent inhibition of NO production. For 9 mol % copolymer, statistically significant anti-inflammatory activity was observed at concentration as low as 10 mg/L. At ~0.1 g/L, the polymers exhibited pronounced activity in suppressing production of NO and achieved this with only negligible change in the cell viability. Administration of even higher doses, 1 g/L, resulted in 80–90% reduction in relative NO levels and this was true for each of the three macromolecular prodrugs. At this concentration, anti-inflammatory activity of the samples with 2 and 6 mol % RBV was accompanied by a significant drop in the cell viability. Remarkably, for 9 mol % sample, near-complete inhibition of production of NO was achieved with only a minor change in the rate of cell proliferation. In other words, using this polymer sample, anti-inflammatory activity well exceeded that of the pristine drug at no expense to the cell viability.

To illustrate the achieved therapeutic benefit quantitatively, Table 1 lists the EC_{50} and IC_{50} values for the synthesized polymers and the pristine drug. The EC_{50} for the non-conjugated drug exceeds the value of IC_{50} by just under a factor of 3 and the difference between these two metrics is ~12 μM, illustrating the discussed above very narrow therapeutic window of RBV in the anti-iNOS treatment in cultured macrophages. The EC_{50} and IC_{50} values for the polymers are listed in units of mass based on dissolved polymer sample and molarity as calculated for equivalent concentrations of RBV. The latter were calculated for a highly unlikely case of complete drug release achieved within the time frame of the experiment. For each of the three polymers, it holds true that EC_{50} value (μM) is higher than that for the pristine drug reflecting a well-documented notion of apparent loss of drug activity largely due to incomplete drug release.[59−62] IC_{50} values of associated toxicity were estimated for polymers A and B by extrapolating a dose−response curve. This was not possible for polymer C as toxicity does not exceed 10% in the studied range, indicating an IC_{50} value far exceeding 1 g/L. Comparing the active and toxic doses (Table 1) makes it apparent that each of the three polymers delivers a significant therapeutic benefit through a tremendously increased therapeutic window. Thus, the therapeutic index (IC_{50}/EC_{50} ratio) is increased to at least 5−18 and the difference in EC_{50} and IC_{50} is increased to millimolar concentrations for the 6 mol % RBV copolymer.

CONCLUSIONS

Ribavirin, a broad-spectrum antiviral and current standard of care against HCV was herein established as an inhibitor of production of nitric oxide in stimulated macrophages. We believe that this constitutes the first detailed investigation of inhibition of nitric oxide synthase using RBV in a setting with relevance to HCV. However, the therapeutic window for this treatment was found to be very narrow, IC_{50}/EC_{50} of 3 and $IC_{50}-EC_{50}$ of 12 μM. Further to this, presented toxicological data for RBV in hepatocytes and macrophages indicated that toxic effects manifest themselves earlier in macrophages than in hepatocytes, a phenomenon that should be taken into account when investigating controlled delivery of RBV. To optimize delivery of RBV, we synthesized macromolecular prodrugs based on a polymer with an extensive history of biomedical applications, PVP. The use of polymer therapeutics afforded a significant therapeutic benefit increasing IC_{50}/EC_{50} ratio to 5−18 and extending the therapeutic window to over 1000 μM. For the copolymer with 9 mol % RBV-containing monomer units, inhibition of NO synthesis well exceeded that achieved with RBV taken at its clinical therapeutic dose and was accompanied with only a minor cytotoxicity. We believe that this report contributes significantly to the understanding of mechanism of action of RBV, a broad spectrum antiviral agent, and delivers a virus-free assay system to monitor activity of this drug or prodrugs derived from it. Most significantly, we developed polymer-conjugated formulations of RBV that deliver significant therapeutic benefit and, thus, contribute to the development of safer treatments against HCV and other viral diseases.

dx.doi.org/10.1021/bm401048s | *Biomacromolecules* 2013, 14, 3916−3926

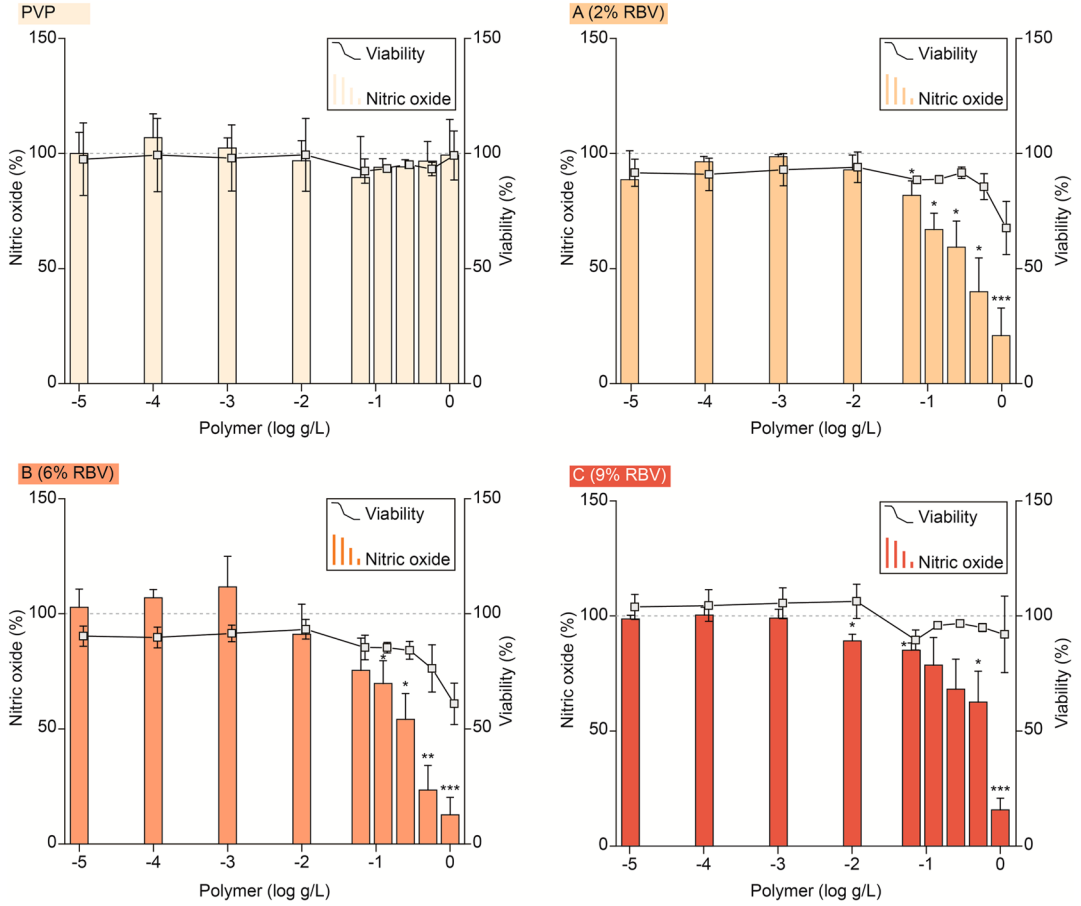

Figure 12. Dose-dependent inhibition of nitric oxide production and accompanying cell viability in LPS-stimulated RAW264.7 cells by PVP-RBV library. Results shown are the average of three independent experiments, reported as mean ± SD (n = 3). Statistical significance is given compared to the negative control. *P < 0.05, **P < 0.01, ***P < 0.001.

Table 1. Comparison of EC_{50} and IC_{50} Values between Free RBV and Macromolecular Prodrugs as Well as Corresponding Therapeutic Indices (IC_{50}/EC_{50})

sample	EC_{50} (g/L)	EC_{50} (μM)	IC_{50} (g/L)	IC_{50} (μM)	IC_{50}/EC_{50}	$IC_{50}-EC_{50}$ (μM)
RBV		7		19	3	12
A (2 mol %)	0.29	51	1.33	232	5	181
B (6 mol %)	0.13	64	2.29	1123	18	1059
C (9 mol %)	0.32	225	>1	>703	>3	>478

■ ASSOCIATED CONTENT

Supporting Information

Activity and toxicity of ribavirin at 48 h preincubation and in confluent cell culture, synthesis scheme of PVP-RBV macromolecular prodrugs, activity and toxicity of MPs after 48 h preincubation, representative ^{1}H NMR illustrating quantification of RBV content, summarized polymer properties. This material is available free of charge via the Internet at http://pubs.acs.org.

■ AUTHOR INFORMATION

Corresponding Author

*E-mail: zelikin@chem.au.dk. Tel.: +45-87155-906.

Funding

This work is supported by a grant from the Lundbeck Foundation and Sapere Aude Starting Grant from the Danish Council for Independent Research, Technology and Production Sciences, Denmark.

Notes

The authors declare no competing financial interest.

■ ACKNOWLEDGMENTS

We would like to thank Kenneth Goldie, University of Basel for investigating TEM imaging. Erythrocytes were supplied generously by the Skejby Hospital blood bank.

■ REFERENCES

(1) WHO. Hepatitis C, 2012; http://www.who.int/mediacentre/factsheets/fs164/en/index.html.

(2) Sharma, P.; Lok, A. Viral hepatitis and liver transplantation. *Semin. Liver Dis.* **2006**, *26* (3), 285−297.

(3) Dore, G. J.; Matthews, G. V.; Rockstroh, J. Future of hepatitis C therapy: Development of direct-acting antivirals. *Curr. Opin. HIV AIDS* **2011**, *6*, 508−513.

(4) Tan, S.-L.; Pause, A.; Shi, Y.; Sonenberg, N. Hepatitis C therapeutics: Current status and emerging strategies. *Nat. Rev. Drug Discovery* **2002**, *1*, 867−881.

(5) Fried, M. W.; Hadziyannis, S. J. Treatment of chronic hepatitis C infection with peginterferons plus ribavirin. *Semin. Liver Dis.* **2004**, *24* (SUPPL. 2), 47−54.

(6) Fried, M. W. Side effects of therapy of hepatitis C and their management. *Hepatology* **2002**, *36* (5B), s237−s244.

(7) Brillanti, S.; Mazzella, G.; Roda, E. Ribavirin for chronic hepatitis C: And the mystery goes on. *Digest. Liver Dis.* **2011**, *43*, 425−430.

(8) Sidwell, R. W.; Huffman, J. H.; Khare, L., G. P.; Allen, B.; Witkowski, R., J. T.; Robins, K. Broad-spectrum antiviral activity of virazole: 1-f8-D-Ribofuranosyl-1,2,4-triazole- 3-carboxamide. *Science* **1972**, *177* (4050), 705−706.
(9) Patterson, J. L.; Fernandez-Larsson, R. Molecular mechanisms of action of ribavirin. *Rev. Infect. Dis.* **1990**, *12* (6), 1139−1146.
(10) Jain, M. K.; Zoellner, C. Role of ribavirin in HCV treatment response: Now and in the future. *Expert Opin. Pharmacother.* **2010**, *11*, 673−683.
(11) De Franceschi, L.; Fattovich, G.; Turrini, F.; Ayi, K.; Brugnara, C.; Manzato, F.; Noventa, F.; Stanzial, A. M.; Solero, P.; Corrocher, R. Hemolytic anemia induced by ribavirin therapy in patients with chronic hepatitis C virus infection: Role of membrane oxidative damage. *Hepatology* **2000**, *31* (4), 997−1004.
(12) Canonico, P. G.; Kastello, M. D.; Spears, C. T.; Brown, J. R.; Jackson, E. A.; Jenkins, D. E. Effects of ribavirin on red blood cells. *Toxicol. Appl. Pharmacol.* **1984**, *74* (2), 155−162.
(13) Brochot, E.; Castelain, S.; Duverlie, G.; Capron, D.; Nguyen-Khac, E.; François, C. Ribavirin monitoring in chronic hepatitis C therapy: Anaemia versus efficacy. *Antiviral Ther.* **2010**, *15* (5), 687−695.
(14) Gilbert, B. E.; Knight, V. Biochemistry and clinical applications of ribavirin. *Antimicrob. Agents Chemother.* **1986**, *30* (2), 201−205.
(15) Naik, G. S.; Tyagi, M. G. A Pharmacological profile of ribavirin and monitoring of its plasma concentration in chronic hepatitis C infection. *J. Clin. Exp. Hepatol.* **2012**, *2* (1), 42−54.
(16) Feld, J. J.; Hoofnagle, J. H. Mechanism of action of interferon and ribavirin in treatment of hepatitis C. *Nature* **2005**, *436*, 967−972.
(17) Hofmann, W. P.; Herrmann, E.; Sarrazin, C.; Zeuzem, S. Ribavirin mode of action in chronic hepatitis C: From clinical use back to molecular mechanisms. *Liver Int.* **2008**, *28*, 1332−1343.
(18) De Clercq, E. Strategies in the design of antiviral drugs. *Nat. Rev. Drug Discovery* **2002**, *1*, 13−25.
(19) Michaelis, M.; Michaelis, R.; Suhan, T.; Schmidt, H.; Mohamed, A.; Doerr, H. W.; Cinatl, J., Jr. Ribavirin inhibits angiogenesis by tetrahydrobiopterin depletion. *FASEB J.* **2007**, *21*, 81−87.
(20) Marletta, M. A. Nitric oxide synthase structure and mechanism. *J. Biol. Chem.* **1993**, *268*, 12231−12234.
(21) Streeter, D. G.; Witkowski, J. T.; Khare, G. P.; Sidwell, R. W.; Bauer, R. J.; Robins, R. K.; Simon, L. N. Mechanism of action of 1-D-ribofuranosyl-1,2,4-triazole-3-carboxamide (Virazole), a new broad-spectrum antiviral agent. *Proc. Natl. Acad. Sci. U.S.A.* **1973**, *70* (4), 1174−1178.
(22) Kast, R. E. Ribavirin in cancer immunotherapies: Controlling nitric oxide augments cytotoxic lymphocyte function. *Neoplasia* **2003**, *5*, 3−8.
(23) Majano, P. L.; Garcia-Monzon, C. Does nitric oxide play a pathogenic role in hepatitis C virus infection? *Cell Death Differ.* **2003**, *10*, S13−S15.
(24) Allison, A. C. Mechanisms of action of mycophenolate mofetil. *Lupus* **2005**, *14*, s2−s8.
(25) Kryger, M. B. L.; Wohl, B. M.; Smith, A. A. A.; Zelikin, A. N. Macromolecular prodrugs of ribavirin combat side effects and toxicity with no loss of activity of the drug. *Chem. Commun.* **2013**, *49* (26), 2643−2645.
(26) Duncan, R. The dawning era of polymer therapeutics. *Nat. Rev. Drug Discovery* **2003**, *2* (5), 347−360.
(27) Li, W.; Chang, Y.; Zhan, P.; Zhang, N.; Liu, X.; Pannecouque, C.; De Clercq, E. Synthesis, in vitro and in vivo release kinetics, and anti-HIV activity of a sustained-release prodrug (mPEG-AZT) of 3′-azido-3′-deoxythymidine (AZT, Zidovudine). *ChemMedChem* **2010**, *5* (11), 1893−1898.
(28) Li, W. J.; Wu, J. D.; Zhan, P.; Chang, Y.; Pannecouque, C.; De Clercq, E.; Liu, X. Y. Synthesis, drug release and anti-HIV activity of a series of PEGylated zidovudine conjugates. *Int. J. Biol. Macromol.* **2012**, *50* (4), 974−980.
(29) Wannachaiyasit, S.; Chanvorachote, P.; Nimmannit, U. A novel anti-HIV dextrin-zidovudine conjugate improving the pharmacokinetics of zidovudine in rats. *AAPS PharmSciTech* **2008**, *9* (3), 840−850.
(30) Wan, L.; Zhang, X.; Gunaseelan, S.; Pooyan, S.; Debrah, O.; Leibowitz, M. J.; Rabson, A. B.; Stein, S.; Sinko, P. J., Novel multicomponent nanopharmaceuticals derived from poly(ethylene) glycol, retro-inverso-Tat nonapeptide and saquinavir demonstrate combined anti-HIV effects. *AIDS Res. Ther.* **2006**, *3*, (1).
(31) Giammona, G.; Cavallaro, G.; Pitarresi, G. Studies of macromolecular prodrugs of zidovudine. *Adv. Drug Delivery Rev.* **1999**, *39* (1−3), 153−164.
(32) Gao, Y.; Katsuraya, K.; Kaneko, Y.; Mimura, T.; Nakashima, H.; Uryu, T. Synthesis of azidothymidine-bound Curdlan sulfate with anti-human immunodeficiency virus activity in vitro. *Polym. J.* **1998**, *30* (1), 31−36.
(33) Li, X.; Wu, Q.; Zhang, F.; Lin, X. F. Chemoenzymatic synthesis, characterization, and controlled release of functional polymeric prodrugs with acyclovir as pendant. *J. Appl. Polym. Sci.* **2008**, *108* (1), 431−437.
(34) Li, X.; Wu, Q.; Chen, Z.; Gong, X.; Lin, X. Preparation, characterization and controlled release of liver-targeting nanoparticles from the amphiphilic random copolymer. *Polymer* **2008**, *49* (22), 4769−4775.
(35) Neeraj, A.; Chandrasekar, M. J. N.; Sara, U. V. S.; Rohini, A. Poly(HEMA-zidovudine) conjugate: A macromolecular pro-drug for improvement in the biopharmaceutical properties of the drug. *Drug Delivery* **2011**, *18* (4), 272−280.
(36) Vlieghe, P.; Clerc, T.; Pannecouque, C.; Witvrouw, M.; De Clercq, E.; Salles, J. P.; Kraus, J. L. Synthesis of new covalently bound κ-carrageenan-AZT conjugates with improved anti-HIV activities. *J. Med. Chem.* **2002**, *45* (6), 1275−1283.
(37) Levy, G. A.; Adamson, G.; Phillips, M. J.; Scrocchi, L. A.; Fung, L.; Biessels, P.; Ng, N. F.; Ghanekar, A.; Rowe, A.; Ma, M. X. Z.; Levy, A.; Koscik, C.; He, W.; Gorczynski, R.; Brookes, S.; Woods, C.; McGilvray, I. D.; Bell, D. Targeted delivery of ribavirin improves outcome of murine viral fulminant hepatitis via enhanced anti-viral activity. *Hepatology* **2006**, *43* (3), 581−591.
(38) Li, X.; Wu, Q.; Lu, M.; Zhang, F.; Lin, X. F. Novel hepatoma-targeting micelles based on chemo-enzymatic synthesis and self-assembly of galactose-functionalized ribavirin-containing amphiphilic random copolymer. *J. Polym. Sci., Polym. Chem.* **2008**, *46* (8), 2734−2744.
(39) Di Stefano, G.; Colonna, F. P.; Bongini, A.; Busi, C.; Mattioli, A.; Fiume, L. Ribavirin conjugated with lactosaminated poly-L-lysine. Selective delivery to the liver and increased antiviral activity in mice with viral hepatitis. *Biochem. Pharmacol.* **1997**, *54* (3), 357−363.
(40) Di Stefano, G.; Bignamini, A.; Busi, C.; Colonna, P. P.; Fiume, L. Enhanced accumulation of ribavirin and its metabolites in liver versus erythrocytes in mice administered with the liver targeted drug. *Italian J. Gastroenterol. Hepatol.* **1997**, *29* (5), 420−426.
(41) Kryger, M. B. L.; Smith, A. A. A.; Wohl, B. M.; Zelikin, A. N. Macromolecular prodrugs for controlled delivery of ribavirin. *Macromol. Biosci.* DOI: 10.1002/mabi.201300244.
(42) Nair, B. Final report on the safety assessment of polyvinylpyrrolidone (PVP). *Int. J. Toxicol.* **1998**, *17* (SUPPL. 4), 95−130.
(43) Kaneda, Y.; Tsutsumi, Y.; Yoshioka, Y.; Kamada, H.; Yamamoto, Y.; Kodaira, H.; Tsunoda, S.; Okamoto, T.; Mukai, Y.; Shibata, H.; Nakagawa, S.; Mayumi, T. The use of PVP as a polymeric carrier to improve the plasma half-life of drugs. *Biomaterials* **2004**, *25* (16), 3259−3266.
(44) Boyer, C.; Bulmus, V.; Davis, T. P.; Ladmiral, V.; Liu, J.; Perrier, S. b. Bioapplications of RAFT polymerization. *Chem. Rev.* **2009**, *109* (11), 5402−5436.
(45) Shimoni, O.; Postma, A.; Yan, Y.; Scott, A. M.; Heath, J. K.; Nice, E. C.; Zelikin, A. N.; Caruso, F. Macromolecule functionalization of disulfide-bonded polymer hydrogel capsules and cancer cell targeting. *ACS Nano* **2012**, *6* (2), 1463−1472.

(46) Zelikin, A. N.; Such, G. K.; Postma, A.; Caruso, F. Poly(vinylpyrrolidone) for bioconjugation and surface ligand immobilization. *Biomacromolecules* **2007**, *8* (9), 2950−2953.
(47) Moorcroft, M. J.; Davis, J.; Compton, R. G. Detection and determination of nitrate and nitrite: A review. *Talanta* **2001**, *54*, 785−803.
(48) Kanuri, G.; Weber, S.; Volynets, V.; Spruss, A.; Bischoff, S. C.; Bergheim, I. Cinnamon extract protects against acute alcohol-induced liver steatosis in mice. *J. Nutr.* **2009**, *139* (3), 482−487.
(49) Markusic, D. M.; van Til, N. P.; Hiralall, J. K.; Elferink, R. P. J. O.; Seppen, J. Reduction of liver macrophage transduction by pseudotyping lentiviral vectors with a fusion envelope from Autographa californica GP64 and Sendai virus F2 domain. *BMC Biotechnol.* **2009**, 9.
(50) Tsubota, A.; Akuta, N.; Suzuki, F.; Suzuki, Y.; Someya, T.; Kobayashi, M.; Arase, Y.; Saitoh, S.; Ikeda, K.; Kumada, H. Viral dynamics and pharmacokinetics in combined interferon alfa-2b and ribavirin therapy for patients infected with hepatitis C virus of genotype 1b and high pretreatment viral load. *Intervirology* **2002**, *45*, 33−42.
(51) Kmoníčková, E.; Potměšil, P.; Holý, A.; Zídek, Z. Purine P1 receptor-dependent immunostimulatory effects of antiviral acyclic analogues of adenine and 2,6-diaminopurine. *Eur. J. Pharmacol.* **2006**, *530* (1−2), 179−187.
(52) Rautio, J.; Kumpulainen, H.; Heimbach, T.; Oliyai, R.; Oh, D.; Jarvinen, T.; Savolainen, J. Prodrugs: design and clinical applications. *Nat. Rev. Drug Discovery* **2008**, *7* (3), 255−270.
(53) Nielsen, A. L.; Steffensen, K.; Larsen, K. L. Self-assembling microparticles with controllable disruption properties based on cyclodextrin interactions. *Colloids Surf., B* **2009**, *73* (2), 267−275.
(54) Ren, S. D.; Chen, D. Y.; Jiang, M. Noncovalently connected micelles based on a β-cyclodextrin-containing polymer and adamantane end-capped poly(ε-caprolactone) via host−guest interactions. *J. Polym. Sci., Polym. Chem.* **2009**, *47* (17), 4267−4278.
(55) Zelikin, A. N.; Becker, A. L.; Johnston, A. P. R.; Wark, K. L.; Turatti, F.; Caruso, F. A general approach for DNA encapsulation in degradable polymer miocrocapsules. *ACS Nano* **2007**, *1* (1), 63−69.
(56) Pissuwan, D.; Boyer, C.; Gunasekaran, K.; Davis, T. P.; Bulmus, V. In vitro cytotoxicity of RAFT polymers. *Biomacromolecules* **2010**, *11* (2), 412−420.
(57) Chang, C.-W.; Bays, E.; Tao, L.; Alconcel, S. N. S.; Maynard, H. D. Differences in cytotoxicity of poly(PEGA)s synthesized by reversible addition-fragmentation chain transfer polymerization. *Chem. Commun.* **2009**, *24*, 3580−3582.
(58) Moncada, S.; Palmer, R. M. J.; Higgs, E. A. Nitric oxide: Physiology, pathophysiology, and pharmacology. *Pharmacol. Rev.* **1991**, *43* (2), 109−142.
(59) Lavignac, N.; Nicholls, J. L.; Ferruti, P.; Duncan, R. Poly(amidoamine) conjugates containing doxorubicin bound via an acid-sensitive linker. *Macromol. Biosci.* **2009**, *9* (5), 480−487.
(60) Kovar, L.; Etrych, T.; Kabesova, M.; Subr, V.; Vetvicka, D.; Hovorka, O.; Strohalm, J.; Sklenar, J.; Chytil, P.; Ulbrich, K.; Rihova, B. Doxorubicin attached to HPMA copolymer via amide bond modifies the glycosylation pattern of EL4 cells. *Tumor Biol.* **2010**, *31* (4), 233−242.
(61) Veronese, F. M.; Schiavon, O.; Pasut, G.; Mendichi, R.; Andersson, L.; Tsirk, A.; Ford, J.; Wu, G. F.; Kneller, S.; Davies, J.; Duncan, R. PEG-doxorubicin conjugates: Influence of polymer structure on drug release, in vitro cytotoxicity, biodistribution, and antitumor activity. *Bioconjugate Chem.* **2005**, *16* (4), 775−784.
(62) Oberoi, H. S.; Laquer, F. C.; Marky, L. A.; Kabanov, A. V.; Bronich, T. K. Core cross-linked block ionomer micelles as pH-responsive carriers for *cis*-diamminedichloroplatinum(II). *J. Controlled Release* **2011**, *153* (1), 64−72.